Electronic Supplementary Material (ESI) for Faraday Discussions.

An evaluation of source apportionment of fine OC and $PM_{2.5}$ by multiple methods: APHH-Beijing campaigns as a case study

Jingsha Xu, Deepchandra Srivastava, Xuefang Wu, Siqi Hou, Tuan V. Vu, Di Liu, Yele Sun, Athanasia Vlachou, Vaios Moschos, Gary Salazar, Sönke Szidat, André S.H. Prévôt, Pingqing Fu, Roy M. Harrison, Zongbo Shi

Supplemental information

Experimental

1 Chemical Mass Balance (CMB) modelling

CMB (US EPA CMB8.2) modelling for IAP and PG sites was conducted separately using the same source profiles mainly obtained from China. Experimental details are provided in Xu et al. (2020) [1] and Wu et al. (2020) [2] for IAP and PG, respectively. The selected main fitting species included EC, n-alkanes (C24-C33), levoglucosan, 17a (H) -22, 29, 30-trisnorhopane, 17b (H), 21a (H) -norhopane, palmitic acid, stearic acid, fluoranthene, phenanthrene, retene, benz(a)anthracene, chrysene, benzo(b)fluoranthene, benzo(k)fluoranthene, benzo[ghi]perylene and picene. Measurement uncertainties of each chemical species have been considered when running the model. In total, seven primary sources including vegetative detritus, biomass burning, gasoline, diesel, industrial coal combustion, residential coal combustion and cooking were considered for CMB modelling.

2 Positive Matrix Factorization (PMF) modelling

PMF modelling was conducted for both filter-based data and for online Aerodyne Aerosol Mass Spectrometer data (AMS-PMF) and Aerosol Chemical Speciation Monitor data (ACSM-PMF).

For filter-based data, 133 samples at both sites in winter and summer were combined for PMF modelling. Detailed information on the principles of PMF receptor modelling can be found elsewhere [3]. Daily $PM_{2.5}$ mass concentration was set as the total variable in the model. 31 species were selected as model input based on the selection criteria that species should have maximum data points above the detection limits and $S/N > 0.2$; major chemical species and specific tracers such as levoglucosan and picene were also selected. The final solution of PMF- 7 factors including coal combustion, traffic, oil combustion, biomass burning, secondary inorganic ions, road and soil dust, was systematically investigated by applying constraints (i.e. *Q*-robust change < 1%) and evaluating factor profiles, temporal trends, and correlations with external tracers, etc. The corresponding $PM_{2.5}$ and OC equivalent mass concentrations of these sources were computed by the PMF model.

An Aerodyne AMS was used to measure non-refractory PM_1 (NR- PM_1) chemical species (organics, Cl^-, NO_3^-, SO_4^{2-} and NH_4^+) in both winter and summer at the IAP site [4]. AMS data analysis details like relative ionization efficiencies of ions and organics are described elsewhere [5]. For the Pinggu site, an Aerodyne ACSM was applied for real-time measurements of NR- PM_1 chemical species in winter. Details regarding the aerosol sampling and data analysis can be found elsewhere [2]. For both sites, PMF was applied to the high-resolution mass spectra of OA and factors like coal combustion OA (CCOA), biomass burning OA (BBOA), hydrocarbon-like OA (HOA), cooking OA (COA), and oxygenated OA (OOA) were identified. The principles and selection of ideal factor numbers are summarized elsewhere [2]. In winter at IAP, 3 primary factors were CCOA, COA and BBOA; and 3 secondary factors of oxidized primary OA (OPOA), less-oxidized OA (LOOOA), and more-oxidized OA (MOOOA) were summed up as OOA. In summer at IAP, 2 primary factors including HOA and COA were identified, and 3 secondary factors of oxygenated OA including OOA1, OOA2, OOA3 were also summed up as OOA. At PG, five factors including BBOA, COA, CCOA, HOA and OOA were obtained. In this study, OA concentrations were also converted to OC using OA/OC ratios obtained in Beijing: 1.38 for COA/COC, 1.35 for CCOA/CCOC, 1.31 for HOA/HOC, 1.58 for BBOA/BBOC, and 1.78 for OOA/OOC [2].

3 ^{14}C analysis

^{14}C in total carbon (TC) and elemental carbon (EC) was examined on 13 IAP samples and 12 PG samples with corrections applied, such as blank filter value correction, nuclear bomb correction, and charring correction for EC. Details regarding the experimental method are described elsewhere [6]. The non-fossil fuel contributions to TC and EC are expressed as TC_{nf} and EC_{nf}, which are determined using the concentrations of TC and EC multiplied by their corresponding non-fossil fractions (f_{NF}). OC_{nf} is determined as the difference of TC_{nf} and EC_{nf}. Fossil fuel contributions are determined by subtracting non-fossil source contributions from TC, EC, and OC. f_{NF} is determined using equation (1) below:

$$f_{NF}=\frac{f_M}{f_{NF,ref}} \qquad (1)$$

Where f_M is the fractions of modern ($^{14}C/^{12}C$). Biomass burning is the only non-fossil source of EC, the $f_{NF,ref}$ of EC is 1.10 [7]. $f_{NF,ref}$ of OC is calculated using the equation below:

$$f_{NF,ref}=p_{bio} \times f_{M,bio} + p_{bb} \times f_{M,bb} \qquad (2)$$

where $f_{M,bb}$ and $f_{M,bio}$ are the detected f_M values of biomass burning (1.10) and biogenic sources (1.023), respectively [7]. p_{bio} and p_{bb} are the proportions of biogenic source and biomass burning in non-fossil source, which are 0.9 and 0.1 in winter and 0.5 and 0.5 in summer [8]. After subtracting non-fossil source contributions from TC, EC, and OC, the rest are fossil fuel contributions.

4 Extended Gelencser (EG) method

Gelencser et al. [9] reported a method to apportion OC and EC to biomass burning, traffic and secondary organic aerosol. In our study, we combined ^{14}C results with OC/EC ratios in different sources to apportion OC to primary OC from fossil fuel, biomass burning, cooking and secondary OC from fossil and non-fossil fuel, and refer to this method as the extended Gelencser (EG) method. The results are not published yet and the details of calculations are provided in the supplemental information; details of the Gelencser and extended Gelencser methods are provided in Table S1 [10]. The uncertainties of the EG method mainly come from the measurement errors and inferred constituent ratios for different sources.

Table S1 comparison of Gelencser method (G method) and the extended Gelencser method (EG method).

	G method	EG method
EC_{bb}	$OC_{bb} \times (EC/OC)_{bb}$	$\approx {}^{b*}EC_{nf}$
EC_f	$EC - EC_{bb}$	measured by ^{14}C
POC_{bb}	$LG \times (OC/LG)_{bb}$	$= EC_{nf} \times (OC/EC)_{bb} = LG \times (OC/LG)_{bb}$
POC_{bio}	$^{a}CE \times (OC/CE)_{bio}$	^{c}Ignored
POC_f	$EC_f \times (OC/EC)_{traffic}$	$EC_f \times (OC/EC)_{f,\ min}$
SOC_f	$^{*}TC_f - OC_f - EC_f$	$^{*}OC_f - POC_f$
SOC_{nf}	$^{*}TC_{nf} - OC_{bb} - OC_{bio} - EC_{bb}$	$^{*}OC_{nf} - POC_{nf} = OC - EC_{nf} \times (OC/EC)_{nf,\ min}$

[a], CE represents concentrations of cellulose;

[b] $EC_{bb} \approx EC_{nf}$, assuming EC from cooking (EC_{ck}) is very low and can be ignored;

[c] assuming OC_{bio} is very low and can be ignored;

Concentrations marked as * are measured by ^{14}C analysis

Calculations [10]:

$EC_{nf} \approx EC_{bb}$, assuming EC from cooking (EC_{ck}) is very low and can be ignored.

$$EC_{nf}=LG\times(OC/LG)_{bb}\times(EC/OC)_{bb} \qquad (3)$$

Referring to the study of LG/MN and LG/GA ratios, there are two main sources of biomass burning: wood burning and straw burning, each of them could be estimated as follow,

$$EC_{bb} = EC_{wood} + EC_{straw} = LG \times f_{wood} \times (OC/LG)_{wood} \times (EC/OC)_{wood} + LG \times f_{straw} \times (OC/LG)_{straw} \times (EC/OC)_{straw} \qquad (4)$$

Where f_{wood} represents the fraction of LG from wood burning, and f_{straw} represents the fraction of LG from straw burning. f_{straw}=1-f_{wood}, assuming other sources of LG are very low and can be ignored. f_{wood} can be obtained by equation (4),

$$\mathrm{f_{wood}} = \frac{\mathrm{EC_{nf}} - \mathrm{LG} \times \mathrm{(OC/LG)_{straw}} \times \mathrm{(EC/OC)_{straw}}}{\left(\mathrm{(OC/LG)_{wood}} \times \mathrm{(EC/OC)_{wood}} - \mathrm{(OC/LG)_{straw}} \times \mathrm{(EC/OC)_{straw}}\right) \times \mathrm{LG}} \tag{5}$$

As f_{wood} should in range of 0~1, it can be used as the limitation of selection EC/OC and OC/LG ratios. POC_{bb} can be calculated once f_{wood}, EC/OC and OC/LG ratios are confirmed.

$$\mathrm{POC_{bb}} = \mathrm{POC_{wood}} + \mathrm{POC_{straw}} = \mathrm{LG} \times \mathrm{f_{wood}} \times \mathrm{(OC/LG)_{wood}} + \mathrm{LG} \times (1 - \mathrm{f_{wood}}) \times \mathrm{(OC/LG)_{straw}} \tag{6}$$

$$\mathrm{POC_f} = \mathrm{EC_f} \times \mathrm{(POC/EC)_f} \tag{7}$$

$(POC/EC)_f$ ratios varied much along with coal combustion conditions, fuel types and even measurement of OC and EC, it is very hard to accurately determine $(POC/EC)_f$ ratios for a given area. Hence, we introduced the lowest $(OC/EC)_f$ ratios as the $(POC/EC)_f$ to estimate POC_f. The determination of the lowest OC/EC_f ratios can be found in Hou et al. [10], which are 4.2, 5.1 for IAP and PG in winter, and 3.6, 2.8 in summer.

$$\mathrm{POC_f} = \mathrm{EC_f} \times \mathrm{(OC/EC)_{f,min}} \tag{8}$$

$$\mathrm{SOC_f} = \mathrm{OC_f} - \mathrm{POC_f} \tag{9}$$

In same way, primary OC from non-fossil sources can be calculated by lowest $(OC/EC)_{nf}$ ratio. And concentrations of secondary OC from non-fossil sources (SOC_{nf}) and OC from cooking (OC_{ck}) can be obtained.

$$\mathrm{POC_{nf}} = \mathrm{EC_{nf}} \times \mathrm{(OC/EC)_{nf,min}} \tag{10}$$

$$\mathrm{SOC_{nf}} = \mathrm{OC_{nf}} - \mathrm{POC_{nf}} \tag{11}$$

$$\mathrm{OC_{ck}} = \mathrm{POC_{nf}} - \mathrm{OC_{bb}} \tag{12}$$

Where $\mathrm{OC_{ck}}$ is estimated assuming primary biogenic OC can be neglected and $\mathrm{(OC/EC)_{ck}}$ is very high with $\mathrm{EC_{ck}}$ ignored.

Supplemental Tables and Figures

Table S2 Source contributions (μg m^{-3} (%OC)) at IAP and PG in winter and summer estimated by CMB

	IAP		PG	
	Winter	Summer	Winter	Summer
OC	21.5±12.3	6.4±2.3	36.5±29.3	10.7±4.9
OC explained	75.7%	56.1%	69.1%	63.4%
Vegetative detritus	0.1 (0.5%)	0.1 (1.7%)	1.5 (2.8%)	0.3 (2.1%)
Biomass burning (wood)	3.8 (17.4%)	0.3 (4.8%)	6.8 (18.1%)	1.1 (10.7%)
Gasoline	2.0 (10.2%)	0.3 (4.9%)	1.0 (3.4%)	0.1 (1.3%)
Diesel	0.5 (1.9%)	0.1 (1.2%)	6.2 (13.7%)	0.6 (6.2%)
Industrial coal combustion	4.9 (22.0%)	1.8 (29.0%)	3.2 (10.2%)	3.8 (34.1%)
Residential coal combustion	2.6 (12.5%)	0.2 (3.3%)	5.7 (19.0%)	0.4 (4.2%)
Cooking	2.2 (10.6%)	0.7 (11.1%)	0.5 (2.0%)	0.5 (4.9%)
Other OC/SOC	5.3 (24.8%)	2.9 (43.9%)	11.7 (30.9%)	3.9 (36.6%)

Table S3 Source contributions of OA and OC (μg m^{-3}) from AMS/ACSM-PMF results at IAP and PG during winter and summer

IAP				PG			
Winter				Winter			
BBOA	6.5±5.8	BBOC	4.1±3.7	BBOA	9.4±8.7	BBOC	5.9±5.5
COA	5.9±4.1	COC	4.3±3.0	COA	6.6±3.6	COC	4.8±2.6
HOA	-	HOC	-	HOA	9.4±7.3	HOC	7.2±5.6
CCOA	6.2±4.4	CCOC	4.6±3.3	CCOA	15.9±11.4	CCOC	11.8±8.5
OOA	18.0±13.2	OOC	10.1±7.4	OOA	12.9±10.3	OOC	7.3±5.8
Summer							
HOA	0.7±0.4	HOC	0.5±0.3				
COA	1.8±1.0	COC	1.3±0.7				
OOA[c]	7.6±3.7	OOC	4.3±2.1				

Table S4 Source contributions of $PM_{2.5}$ and OC (μg m^{-3}) from PMF results at IAP and PG during winter and summer

	IAP				PG			
	Winter		Summer		Winter		Summer	
	$PM_{2.5}$	OC	$PM_{2.5}$	OC	$PM_{2.5}$	OC	$PM_{2.5}$	OC

Secondary Inorganics	17.5±17.9	1.7±1.7	11.1±11.6	1.1±1.1	21.9±31.1	2.1±3.0	13.2±9.8	1.3±0.9
Coal combustion	16.0±13.7	10.4±8.9	0.6±1.0	0.4±0.6	19.4±19.1	12.6±12.4	4.6±2.1	3.0±1.4
Traffic	7.4±7.3	0.7±0.7	1.7±1.7	0.2±0.2	4.1±4.9	0.4±0.4	1.0±1.0	0.1±0.1
Oil combustion	1.4±1.8	0.3±0.4	1.6±1.9	0.4±0.5	7.1±6.3	1.7±1.5	2.4±2.2	0.6±0.5
Biomass burning	29.0±20.3	3.1±2.2	0.5±0.6	0.1±0.1	27.3±24.9	2.9±2.7	0.2±0.5	0.02±0.1
Dust	9.1±6.2	3.6±2.3	12.5±4.8	4.7±1.9	12.3±11.3	4.7±4.3	6.2±3.8	2.6±1.6
Sum	80.4±47.4	19.8±11.2	28.0±14.1	6.8±2.2	92.1±67.5	24.5±14.5	27.7±12.7	7.6±2.8

Table S5 Source apportionment of OC (μg m^{-3}) by extended Gelencser method

		POC_{bb}	POC_{ck}	POC_{f}	SOC_{nf}	SOC_{f}
IAP	Winter	2.7±1.3	1.1±0.7	10.5±6.2	4.8±2.8	7.7±4.2
	Summer	0.6±0.7	1.1±0.4	2.3±0.8	2.2±2.1	2.0±0.9
PG	Winter	4.8±2.4	5.8±3.6	16.0±7.8	9.1±9.0	13.3±10.4
	Summer	2.0±0.8	0.9±0.4	3.3±1.9	3.1±3.2	2.2±1.6

Table S6 Relative abundance of source contributions (%) at IAP and PG during haze and non-haze days estimated by CMB

	PG winter		IAP winter		IAP summer	
	Haze (n=15)	Non-haze (n=7)	Haze (n=18)	Non-haze (n=13)	Haze (n=1)	Non-haze (n=33)
SNA	27.2*	15.8	38.0	28.7	65.9	48.0
Geological minerals	2.3	4.8	6.3	7.8	7.0	10.6
Vegetative Detritus	2.4	1.6	0.2	0.4	0.3	0.7
Biomass Burning	14.8	14.3	10.2	12.1	0.6	2.2
Gasoline	2.0	3.3	4.9	8.8	1.0	2.3
Diesel	10.3	5.8	1.3	0.6	0.0	0.4
Industrial CC	8.0	8.5	14.9	12.3	7.2	13.3
Residential CC	9.8	21.6	6.8	8.8	1.1	1.4
Cooking	0.5	1.6	3.9	3.9	1.5	2.8
Other OM	22.7	22.8	13.5	16.6	15.3	18.4

* The relative abundance of source contributions was calculated as the source contribution (μg m^{-3}) divided by the sum of all sources’ contributions in percentage.

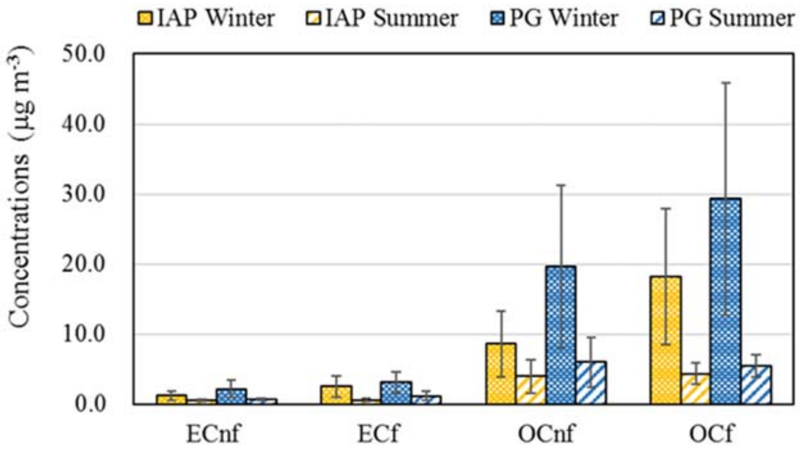

Fig. S1 Fossil and non-fossil fuel derived OC and EC concentrations in winter and summer of IAP and PG sites

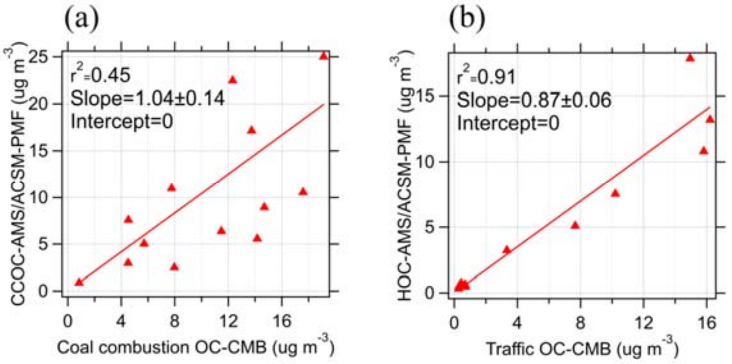

Fig. S2 Correlations of coal combustion (a) and traffic (b) related POC estimated by CMB and AMS/ACSM-PMF.

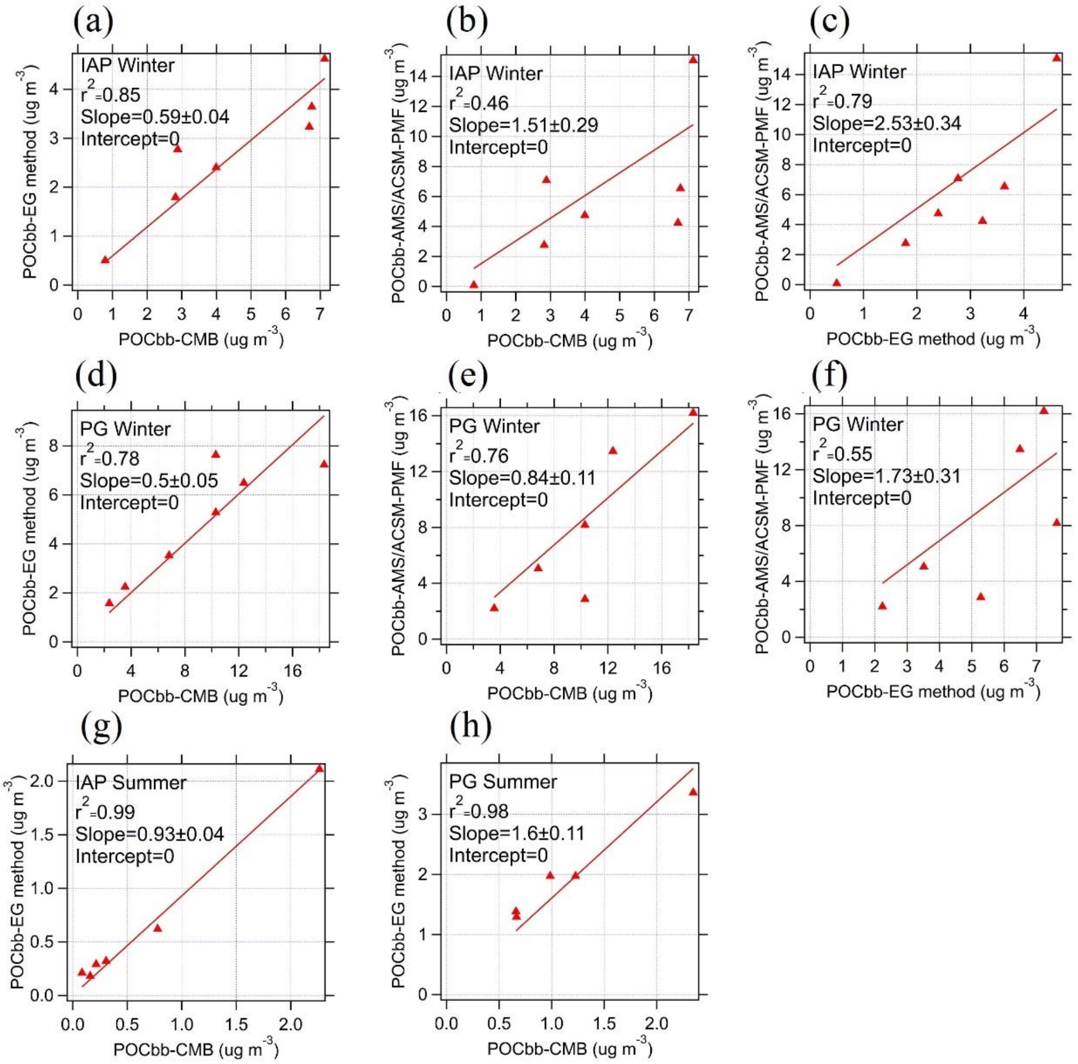

Fig. S3 Comparison of primary OC from biomass burning (POC_{bb}) by different methods in Beijing: (a) Extended Gelencser (EG) method vs CMB at IAP during winter; (b) AMS/ACSM-PMF vs CMB at IAP during winter; (c) AMS/ACSM-PMF vs EG method at IAP during winter; (d) EG method vs CMB at PG during winter; (e) AMS/ACSM-PMF vs CMB at PG during winter; (f) AMS/ACSM-PMF vs EG method at PG during winter; (g) EG method vs CMB at IAP during summer; (h) EG method vs CMB at PG during summer.

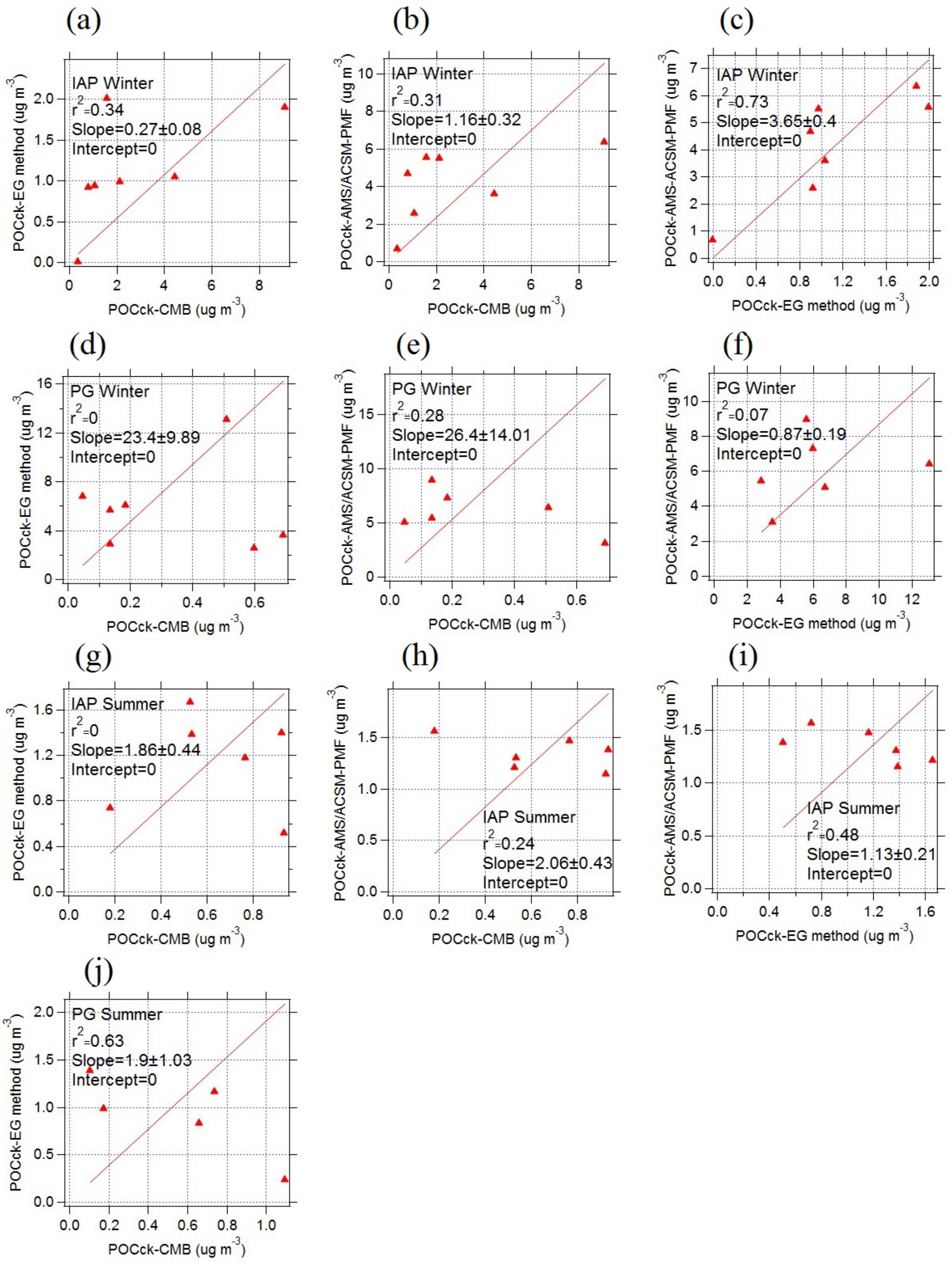

Fig. S4 Comparison of primary OC from cooking (POC_{ck}) by different methods in Beijing: (a) Extended Gelencser (EG) method vs CMB at IAP during winter; (b) AMS/ACSM-PMF vs CMB at IAP during winter; (c) AMS/ACSM-PMF vs EG method at IAP during winter; (d) EG method vs CMB at PG during winter; (e) AMS/ACSM-PMF vs CMB at PG during winter; (f) AMS/ACSM-PMF vs EG method at PG during winter; (g) EG method vs CMB at IAP during summer; (h) AMS/ACSM-PMF vs CMB at IAP during summer; (i) AMS/ACSM-PMF vs EG method at IAP during summer; (j) EG method vs CMB at PG during summer;

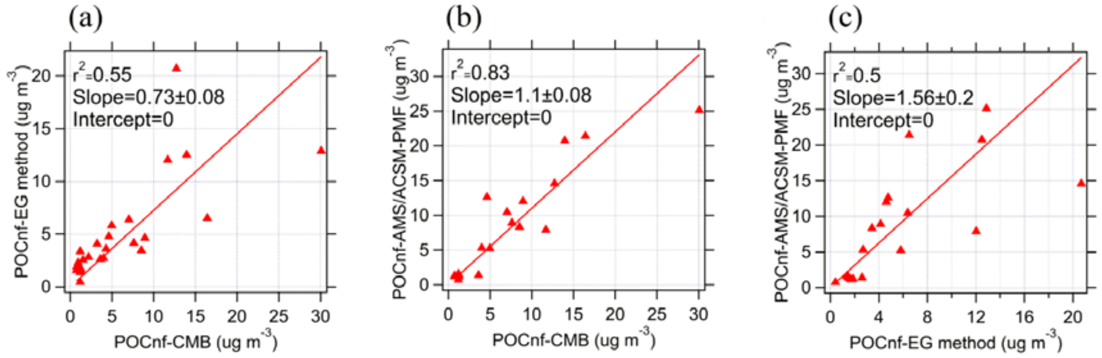

Fig. S5 Correlations of POC$_{nf}$ estimated by different methods: (a) Extended Gelencser (EG) method vs CMB; (b) AMS/ACSM-PMF vs CMB; (c) AMS/ACSM-PMF vs EG method;

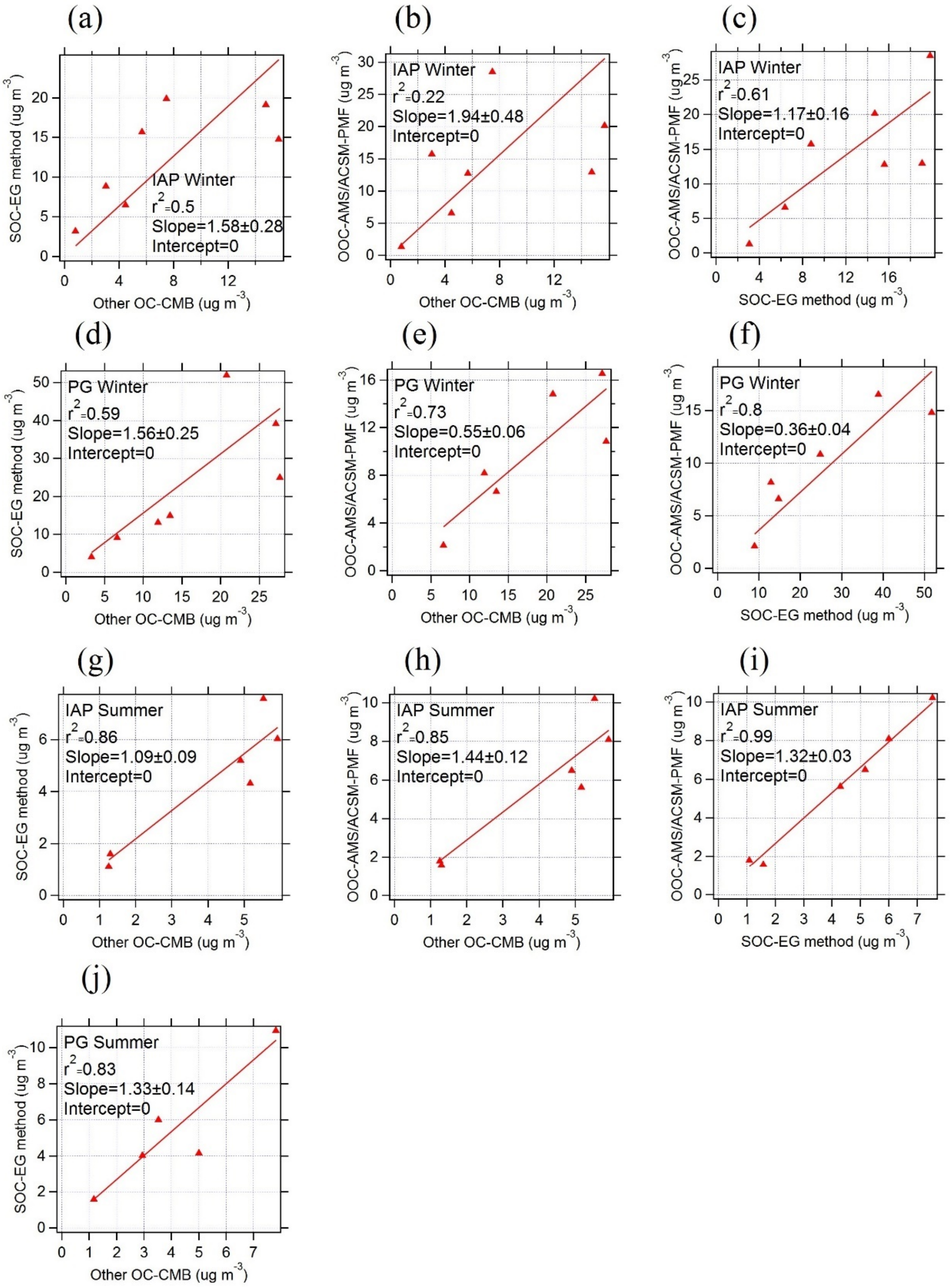

Fig. S6 Comparison of secondary OC (SOC) by different methods in Beijing: (a) Extended Gelencser (EG) method vs CMB at IAP during winter; (b) AMS/ACSM-PMF vs CMB at IAP during winter; (c) AMS/ACSM-PMF vs EG method at IAP during winter; (d) EG method vs CMB at PG during winter; (e) AMS/ACSM-PMF vs CMB at PG during winter; (f) AMS/ACSM-PMF vs EG method at PG during winter; (g) EG method vs CMB at IAP during summer; (h) AMS/ACSM-PMF vs CMB at IAP during summer; (i) AMS/ACSM-PMF vs EG method at IAP during summer; (j) EG method vs CMB at PG during summer;

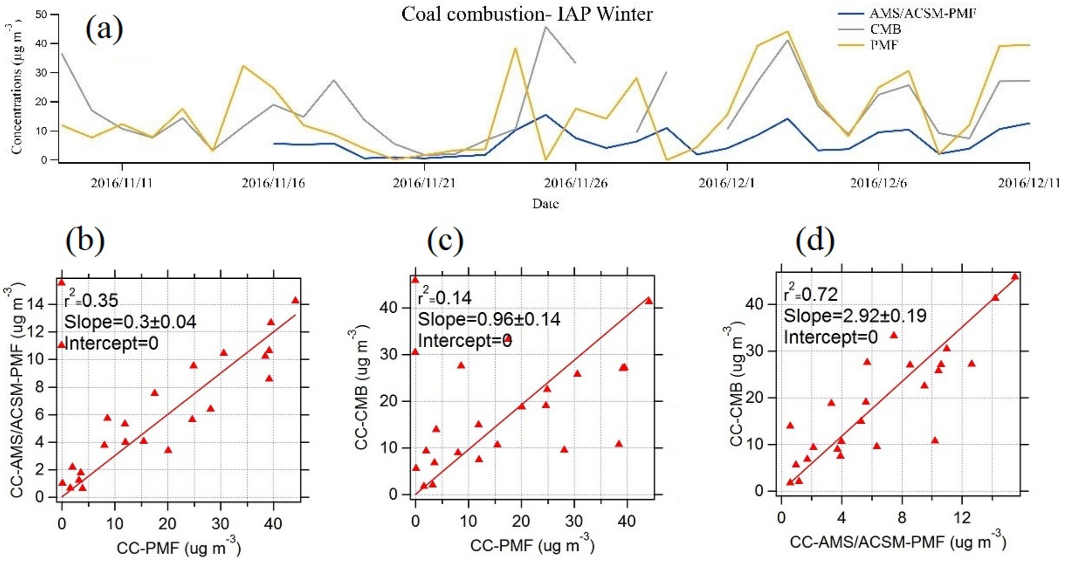

Fig. S7 Time series (a) and correlations of coal combustion (CC) related OM by different methods at IAP during winter: (b) AMS/ACSM-PMF vs PMF; (c) CMB vs PMF; (d) CMB vs AMS/ACSM-PMF;

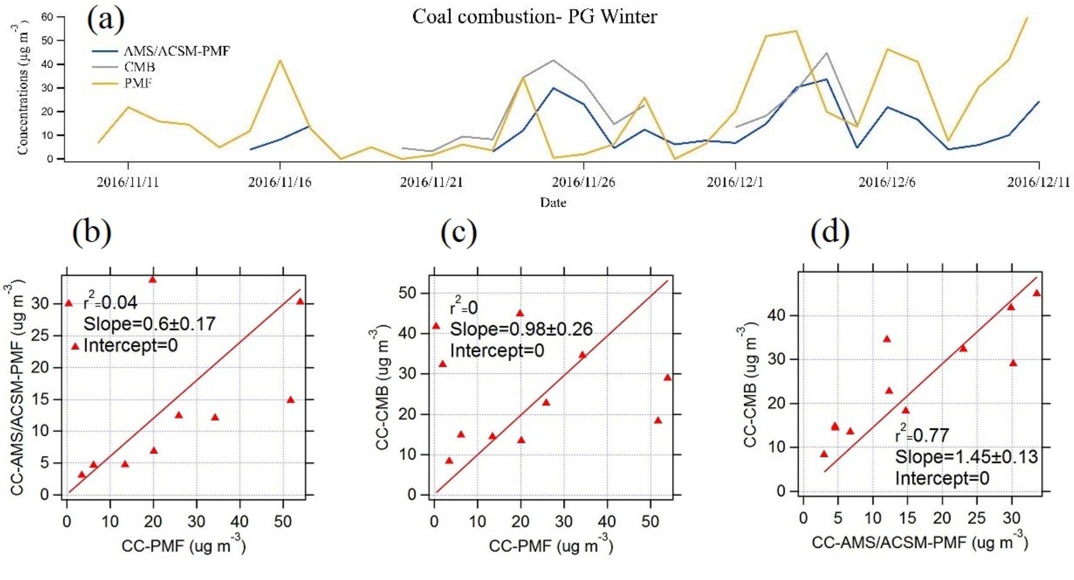

Fig. S8 Time series (a) and correlations of coal combustion (CC) related OM by different methods at PG during winter: (b) AMS/ACSM-PMF vs PMF; (c) CMB vs PMF; (d) CMB vs AMS/ACSM-PMF;

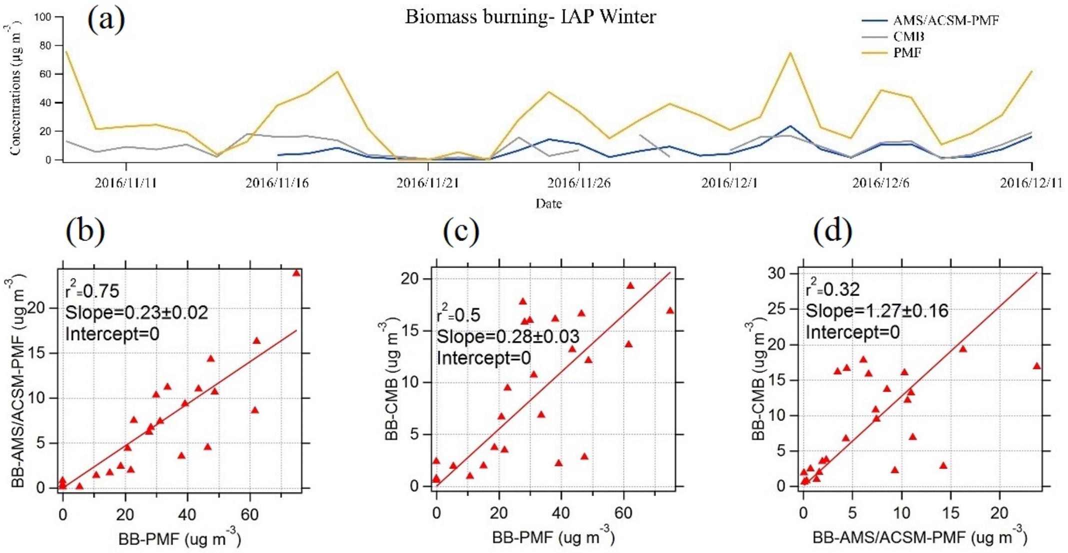

Fig. S9 Time series (a) and correlations of biomass burning (BB) related OM by different methods at IAP during winter: (b) AMS/ACSM-PMF vs PMF; (c) CMB vs PMF; (d) CMB vs AMS/ACSM-PMF;

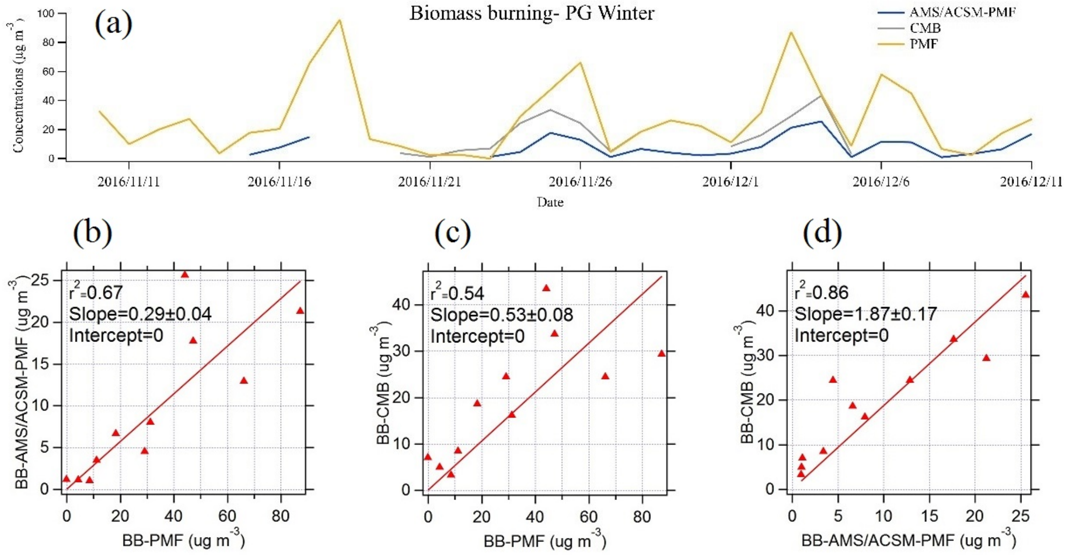

Fig. S10 Time series (a) and correlations of biomass burning (BB) related OM by different methods at PG during winter: (b) AMS/ACSM-PMF vs PMF; (c) CMB vs PMF; (d) CMB vs AMS/ACSM-PMF;

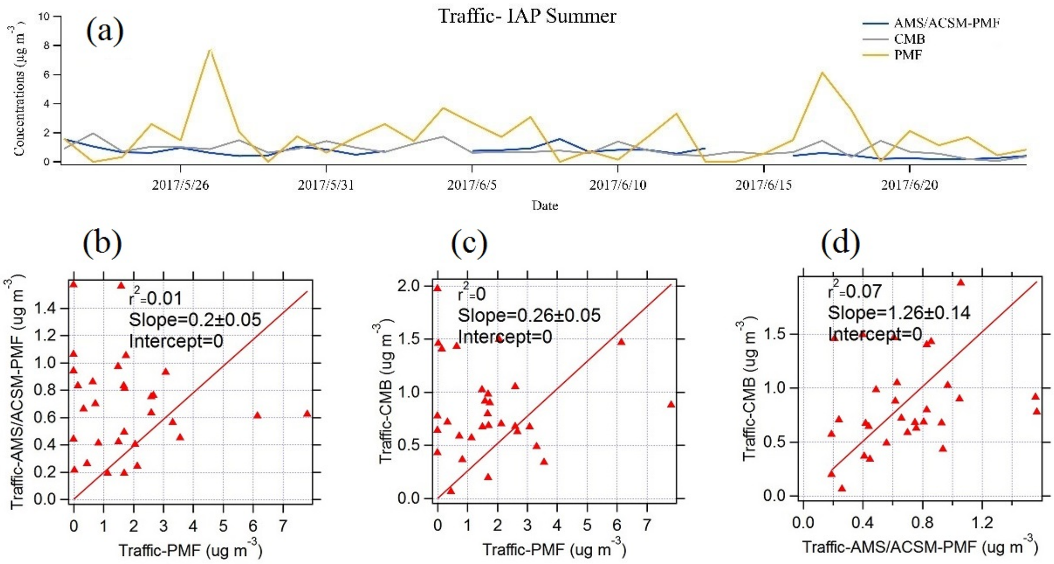

Fig. S11 Time series (a) and correlations of traffic related OM by different methods at IAP during summer: (b) AMS/ACSM-PMF vs PMF; (c) CMB vs PMF; (d) CMB vs AMS/ACSM-PMF;

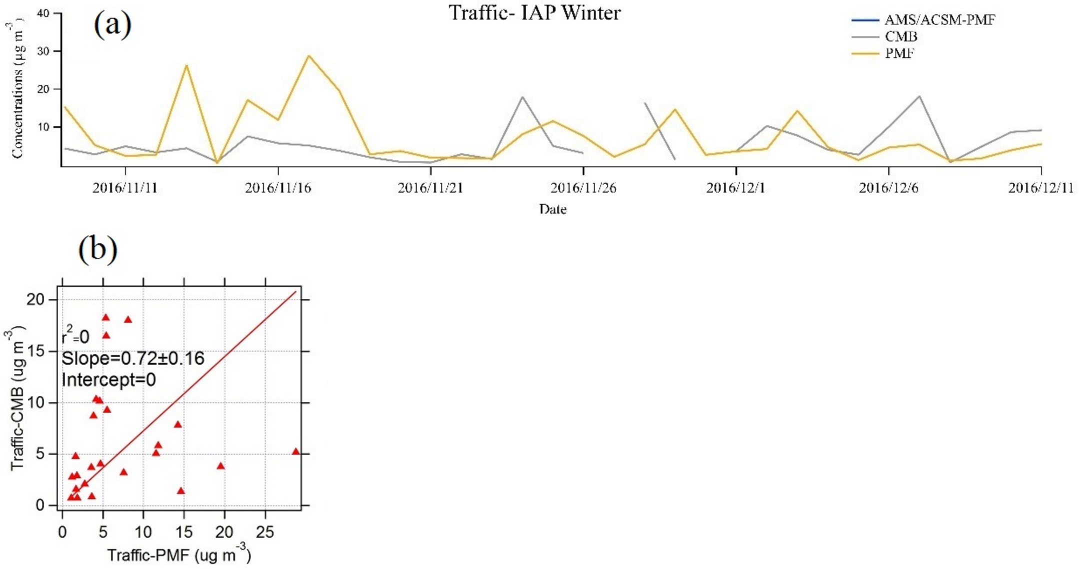

Fig. S12 Time series (a) and correlations of traffic related OM by PMF and CMB (b) at IAP during winter.

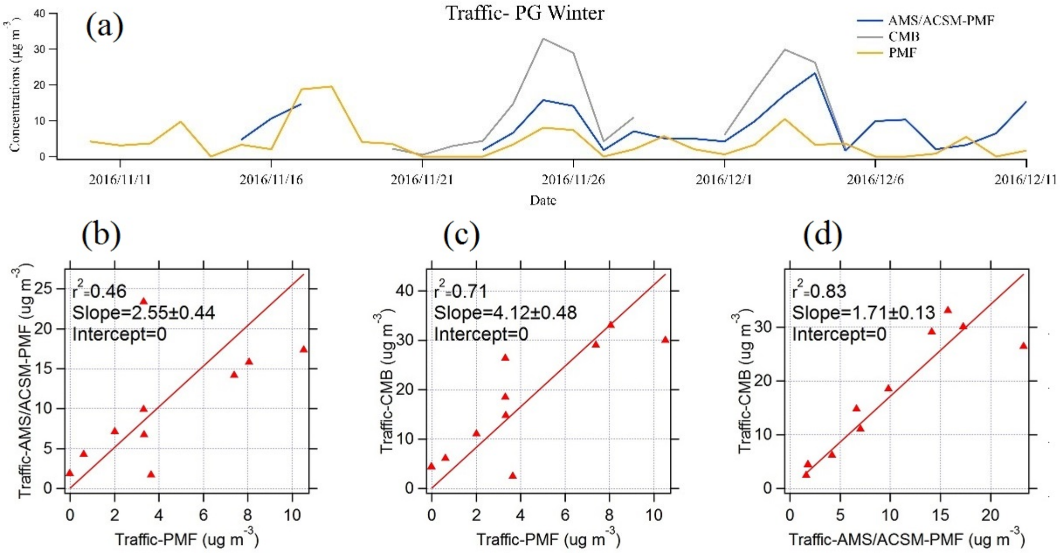

Fig. S13 Time series (a) and correlations of traffic related OM by different methods at PG during winter: (b) AMS/ACSM-PMF vs PMF; (c) CMB vs PMF; (d) CMB vs AMS/ACSM-PMF;

References

1. J. Xu, D. Liu, T. V. Vu, Y. Z. Zhang, P. Fu, Y. Sun, W. Xu, R. M. Harrison and Z. Shi, *Atmospheric Chemistry and Physics (under review)*, 2020.
2. X. Wu, C. Chen, T. V. Vu, D. Liu, C. Baldo, X. Shen, Q. Zhang, K. Cen, M. Zheng, K. He, Z. Shi and R. M. Harrison, *Environmental Pollution (under review)*, 2020.
3. P. Paatero and U. Tapper, *Environmetrics*, 1994, **5**, 111-126.
4. Y. Sun, Y. He, Y. Kuang, W. Xu, S. Song, N. Ma, J. Tao, P. Cheng, C. Wu, H. Su, Y. Cheng, C. Xie, C. Chen, L. Lei, Y. Qiu, P. Fu, P. Croteau and D. R. Worsnop, *Geophysical Research Letters*, 2020, **n/a**, e2019GL086288.
5. W. Xu, Y. Sun, Q. Wang, J. Zhao, J. Wang, X. Ge, C. Xie, W. Zhou, W. Du, J. Li, P. Fu, Z. Wang, D. R. Worsnop and H. Coe, *Journal of Geophysical Research: Atmospheres*, 2019, **124**, 1132-1147.
6. A. Vlachou, K. R. Daellenbach, C. Bozzetti, B. Chazeau, G. A. Salazar, S. Szidat, J. L. Jaffrezo, C. Hueglin, U. Baltensperger, I. E. Haddad and A. S. H. Prévôt, *Atmos. Chem. Phys.*, 2018, **18**, 6187-6206.
7. C. W. Lewis, G. A. Klouda and W. D. Ellenson, *Atmospheric Environment*, 2004, **38**, 6053-6061.
8. I. Levin, T. Naegler, B. Kromer, M. Diehl, R. J. Francey, A. J. Gomez-Pelaez, L. P. Steele, D. Wagenbach, R. Weller and D. E. Worthy, *Tellus B*, 2010, **62**, 26-46.
9. A. Gelencsér, B. May, D. Simpson, A. Sánchez-Ochoa, A. Kasper-Giebl, H. Puxbaum, A. Caseiro, C. Pio and M. Legrand, *Journal of Geophysical Research: Atmospheres*, 2007, **112**.
10. S. Hou, D. Liu, J. Xu, T. V. Vu, X. Wu, D. Srivastava, P. Fu, Y. Sun, A. Vlachou, V. Moschos, G. Salazar, S. Szidat, A. S. H. Prévôt, Z. Shi and R. M. Harrison, 2020.